Available online at www.sciencedirect.com
SCIENCE DIRECT®
International Journal of Thermal Sciences 42 (2003) 447–453
International Journal of Thermal Sciences
www.elsevier.com/locate/ijts

Effect of thermal and mass buoyancy forces on the development of laminar mixed convection between vertical parallel plates with uniform wall heat and mass fluxes

M.M. Salah El-Din

P.O. Box 2574, Al-Sarai 21411, Alexandria, Egypt

Received 10 December 2001; accepted 19 June 2002

Abstract

The effect of thermal and mass buoyancy forces on the development of laminar mixed convection between two vertical parallel plates with uniform heat and mass fluxes has been investigated numerically. Velocity, temperature and concentration profiles have been presented. The effect of the different parameters on heat and mass transfer between the plates has been discussed for positive and negative values of the buoyancy ratio, N. The results showed that positive N increases the Nusselt number and Sherwood number, while negative N decreases them. Schmidt number has the highest effect on the Nusselt number and Sherwood number.

Keywords: Parallel plates; Heat transfer; Mass transfer; Developing flow; Asymmetric heating

1. Introduction

Many analyses of laminar convection in vertical parallel-plates channels are available in the literature. These analyses can be classified into free convection and mixed convection, symmetric and asymmetric heating with uniform wall temperatures or uniform wall heat fluxes. Generally, the developing flow is analyzed by numerical techniques [1–9], while the fully developed flow is analyzed analytically [10–14]. Experimental work is also available [15,16].

The combined effect of thermal and mass buoyancy forces on laminar convection in vertical parallel-plates channels has received less attention. However, it is encountered in many practical situations, such as in the design of heat exchangers, solar energy collectors, thermo-protection systems and many chemical processes. Nelson and Wood have presented numerical analyses of developing laminar flow between vertical parallel-plates for combined heat and mass transfer natural convection with uniform temperature and concentration [17] and uniform heat and mass flux boundary conditions [18]. They also have presented an analytical solution for the fully developed flow [19]. Lee et al. [20] have studied, experimentally and numerically, free convection in a vertical channel within which the buoyancy force reverses its sign. The channel consists of two walls, one porous and the other solid. Mass transfer from the porous wall resulted in a downward flow while heat transfer on the solid wall resulted in an opposing upward flow. Yan et al. [21] have investigated the effect of latent heat transfer, in association with the evaporation of a thin liquid film on the walls of a vertical parallel-plates channel, on the natural convection heat and mass transfer. Desrayaud and Lauriat [22] have examined the condensation of humid air in a vertical parallel plate channel under the same assumption of thin liquid film. The effect of finite film thickness on the heat and mass transfer in natural convection flows has been numerically investigated by Yan and Lin [23] and Yan [24]. Cherif and Daif [25] have confirmed the importance of the film thickness on the heat and mass transfer when a binary mixture (ethanol–water or ethylene glycol–water) flows through a vertical channel whose one dry and adiabatic wall and the other is wet and heated uniformly. Lee [26] has performed an investigation of natural convection heat and mass transfer in open vertical parallel plates with unheated entry and unheated exit. He has demonstrated that the presence of unheated entry and unheated exit severely affects the heat and mass transfer rates.

E-mail address: msalaheldin@netscape.net (M.M. Salah El-Din).

1290-0729/02/$ – see front matter
doi:10.1016/S1290-0729(02)00045-5

Nomenclature

b	channel width	m	
c	species concentration	$kg \cdot m^{-3}$	
C	dimensionless concentration		
D	mass diffusivity	$m^2 \cdot s^{-1}$	
g	gravitational acceleration	$m \cdot s^{-2}$	
Gr	Grashof number, $= g\beta q_1 b^4/\nu^2 k$		
Gr_m	mass Grashof number, $= g\beta_m m_1 b^4/\nu^2 D$		
h	convective heat transfer coefficient	$W \cdot m^{-2} \cdot K^{-1}$	
h_m	convective mass transfer coefficient	$m \cdot s^{-1}$	
k	thermal conductivity	$W \cdot m^{-1} \cdot K^{-1}$	
m	mass flux	$kg \cdot s^{-1} \cdot m^{-2}$	
n	number of grid points in the Y-direction		
N	buoyancy ratio, $= Gr_m/Gr$		
Nu	Nusselt number, $= hb/k$		
p	pressure difference, $= p' - p''$	Pa	
p'	static pressure	Pa	
p''	hydrostatic pressure	Pa	
P	dimensionless pressure difference		
Pr	Prandtl number, $= \nu/\alpha$		
q	heat flux	$W \cdot m^{-2}$	
r_h	heat fluxes ratio, $= q_2/q_1$		
r_m	mass fluxes ratio, $= m_2/m_1$		
Re	Reynolds number, $= u_0 b/\nu$		
Sc	Schmidt number, $= \nu/D$		
Sh	Sherwood number, $= h_m b/D$		
T	temperature	K	
u	axial velocity	$m \cdot s^{-1}$	
v	transverse velocity	$m \cdot s^{-1}$	
x	axial coordinate	m	
y	transverse coordinate	m	

Greek symbols

α	thermal diffusivity	$m^2 \cdot s^{-1}$
β	volumetric coefficient of thermal expansion	K^{-1}
β_m	volumetric coefficient of concentration expansion	$m^3 \cdot kg^{-1}$
γ	dimensionless pressure gradient	
θ	dimensionless temperature	
ν	kinematic viscosity	$m^2 \cdot s^{-1}$
ρ	density	$kg \cdot m^{-3}$

Subscripts

0	value at the entrance
1	value on hot plate
2	value on cool plate

It is noted in the above reviews that the effect of thermal and mass buoyancy forces on the development of laminar forced flow between two vertical parallel plates has not received sufficient attention. In a previous work [27] such effect on fully developed laminar forced convection in a vertical channel has been studied. The channel has different constant wall temperatures and concentrations, which are higher than those at the entrance. Criteria for the occurrence of flow reversal were also presented. The fully developed flow can only be established if the channel is very long. *Pr* and *Sc* have no effect on the bulk temperature and concentration and the location where flow reversal occurs is not evident. Yan [28] has studied the developing laminar mixed convection heat and mass transfer in inclined rectangular ducts. The duct walls are subjected to a constant temperature and concentration. Therefore, the present work is devoted to study the effect of thermal and mass buoyancy forces on the development of laminar mixed convection between two vertical parallel plates in the case of prescribed wall heat and mass fluxes. To the knowledge of the author, this case has not been studied before.

2. Analysis

Consider laminar two-dimensional steady flow between vertical plates. The fluid properties are assumed to be constant except for the buoyancy term of the momentum equation. The flow is incompressible and has a uniform upward vertical velocity at the entrance. The plates have different uniform heat and mass fluxes. The geometry and boundary conditions are shown in Fig. 1.

For many processes in air molecular weights of the mixture are not too different and concentrations are low. Also, temperature differences and pressure drops are small. Under these conditions thermal and pressure diffusions can

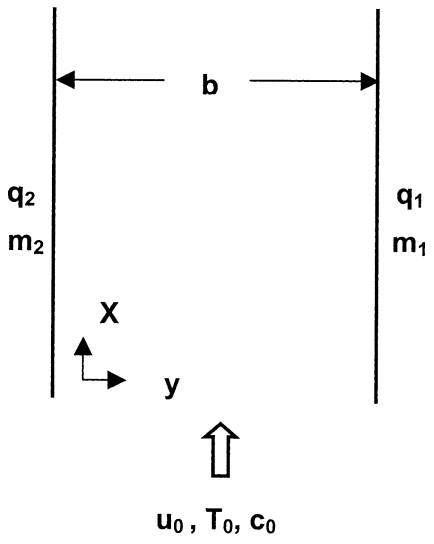

Fig. 1. Geometry and boundary conditions.

be neglected. Diffusion of energy due to concentration gradient may also be neglected.

The dimensionless governing equations, expressing the above conditions, are

Continuity

$$\frac{\partial U}{\partial X}+\frac{\partial V}{\partial Y}=0 \tag{1}$$

x momentum

$$U\frac{\partial U}{\partial X}+V\frac{\partial U}{\partial Y}=-\frac{\partial P}{\partial X}+\frac{\partial^2 U}{\partial Y^2}+\frac{Gr}{Re}(\theta+NC) \tag{2}$$

y momentum

$$\frac{\partial P}{\partial Y}=0 \tag{3}$$

Energy

$$U\frac{\partial \theta}{\partial X}+V\frac{\partial \theta}{\partial Y}=\frac{1}{Pr}\frac{\partial^2 \theta}{\partial Y^2} \tag{4}$$

Mass

$$U\frac{\partial C}{\partial X}+V\frac{\partial C}{\partial Y}=\frac{1}{Sc}\frac{\partial^2 C}{\partial Y^2} \tag{5}$$

where

$$X=\frac{x}{b\,Re},\qquad Y=\frac{y}{b}$$

$$U=\frac{u}{u_0},\qquad V=\frac{bv}{\nu}$$

$$\theta=\frac{T-T_0}{q_1 b/k},\qquad C=\frac{c-c_0}{m_1 b/D}$$

$$P=\frac{p}{\rho u_0^2},\qquad Re=\frac{u_0 b}{\nu}$$

$$Gr=\frac{g\beta q_1 b^4}{\nu^2 k},\qquad N=\frac{Gr_m}{Gr}$$

$$Gr_m=\frac{g\beta_m m_1 b^4}{\nu^2 D}$$

$$Pr=\frac{\nu}{\alpha},\qquad Sc=\frac{\nu}{D}$$

The boundary conditions are

$$X=0,\ 0<Y<1\text{: } U=1,\ V=0,\ \theta=0,\ C=0$$

$$X\geqslant 0,\ Y=0\text{: } U=0,\ V=0,\ \frac{\partial\theta}{\partial Y}=-r_h,\ \frac{\partial C}{\partial Y}=-r_m$$

$$X\geqslant 0,\ Y=1\text{: } U=0,\ V=0,\ \frac{\partial\theta}{\partial Y}=1,\ \frac{\partial C}{\partial Y}=1$$

$$X=0\text{: } P=0$$

Where

$$r_h=\frac{q_2}{q_1},\qquad r_m=\frac{m_2}{m_1}$$

The local Nusselt numbers are

$$Nu_1=\frac{1}{\theta_1},\qquad Nu_2=\frac{r_h}{\theta_2}$$

The local Sherwood numbers are

$$Sh_1=\frac{1}{C_1},\qquad Sh_2=\frac{r_m}{C_2}$$

Conservation of mass at any cross section in the channel gives

$$\int_0^1 U\,\mathrm{d}y=1 \tag{6}$$

3. Method for numerical solution

The governing equations formulated above were solved numerically using a forward-marching, line-by-line implicit finite-difference technique similar to that described by Bodoia and Osterle [1]. Because of the stability and accuracy of this method, many other researchers used it [2,5,6,17]. The solution of the difference equations is obtained by first selecting values for Gr/Re, Pr, Sc, r_h, r_c and N. Then, by means of a marching procedure the variables U, V, θ, C and P for each row are obtained using the values at the previous row.

For uniform heat and mass fluxes, the wall temperatures and concentrations are not specified at the plates. Therefore, the solutions are obtained by successive approximations similar to that described by Aung et al. [2]. First, the plate temperatures and concentrations of any row are set equal to those on the previous row. Hence, solutions for the interior points are obtained. Then, by means of a three-point derivative formula, new plate temperatures and concentrations are computed. With these, new solutions for the interior points are obtained. The procedure is continued until convergence. The obtained temperature and concentration values are then used in the solution of the momentum equation.

To calculate the transverse component of velocity V, Aung et al. [2] integrated the continuity equation from each plate out to within one node of either side of the centerline. The centerline node value was calculated by interpolation. Because of the asymmetry of the problem, it is more convenient to obtain two solutions by integrating from one plate to the other and then in the reverse order [5, 17]. Adding the two solutions together, each weighted by the distance from the plate from which it was calculated, gives the final transverse velocity field. This way was also followed in this work.

Eq. (6) is solved numerically by means of Simpson's rule.

A uniform grid in the Y-direction is used with 51 grid points. The grid size increases in the X-direction as follows:

$$0<X\leqslant 0.001\text{: } \Delta X=0.00005$$

$$0.001<X\leqslant 0.005\text{: } \Delta X=0.0002$$

$$0.005<X\leqslant 0.02\text{: } \Delta X=0.0003$$

$$0.02<X\leqslant 0.1\text{: } \Delta X=0.0005$$

$$X>0.1\text{: } \Delta X=0.005$$

Grid refinement tests were carried out to ensure the independence of the calculations on the grid size. Table 1 presents

Table 1
Effect of grid size in the Y-direction on the local Nusselt numbers. ($Gr/Re = 300,\ Pr = Sc = 0.7,\ r_h = r_c = 0.5,\ N = 1$)

(a) Effect on Nu_1

n	X				
	0.002	0.005	0.02	0.05	0.1
31	11.822	7.503	4.412	3.225	2.393
41	11.399	7.337	4.367	3.206	2.386
51	11.113	7.228	4.339	3.192	2.382
61	10.891	7.141	4.312	3.179	2.379

(b) Effect on Nu_2

n	X				
	0.002	0.005	0.02	0.05	0.1
31	11.708	7.258	4.002	2.719	1.779
41	11.274	7.088	3.955	2.699	1.776
51	10.982	6.975	3.922	2.681	1.774
61	10.756	6.885	3.890	2.664	1.773

the results of the local Nusselt numbers (or Sherwood numbers) for four numbers of grid points in the Y-direction. The table shows that the variations of the Nusselt numbers decrease as the number of grid points increases. It is found that the deviations in Nu_1 and Nu_2 calculated with $n = 51$ and $n = 61$ are always less than ∼2%. Therefore, the calculations with $n = 51$ will be considered sufficiently accurate in the present work. Furthermore, the calculations were carried out for the developing flow without buoyancy forces. For this case, the fully developed solution gives $\gamma = -12$. The calculations give the following results at large values of X:

At $X = 0.5,\ \gamma = -11.99980$

At $X = 1,\ \gamma = -11.99989$

This confirms the accuracy and convergence of the numerical computations along the channel.

4. Results and discussion

The numerical calculations of air ($Pr = 0.7$) in the present study are carried out for different values of the buoyancy ratio N between -0.8 and 2.0 [28]. The buoyancy ratio N represents the ratio between mass and thermal buoyancy forces. When $N = 0$, there is no mass transfer and the buoyancy force is due to the thermal diffusion only. $N > 0$ means that mass buoyancy force acts in the same direction of thermal buoyancy force, while $N < 0$ means that mass buoyancy force acts in the opposite direction.

In the following sections the developments of velocity, temperature and concentration profiles will be presented first, beside the pressure gradient between the plates because of their usefulness in clarification of the heat and mass transfer mechanisms between the plates. Then, the effect of various parameters on the Nusselt and Sherwood numbers will be presented.

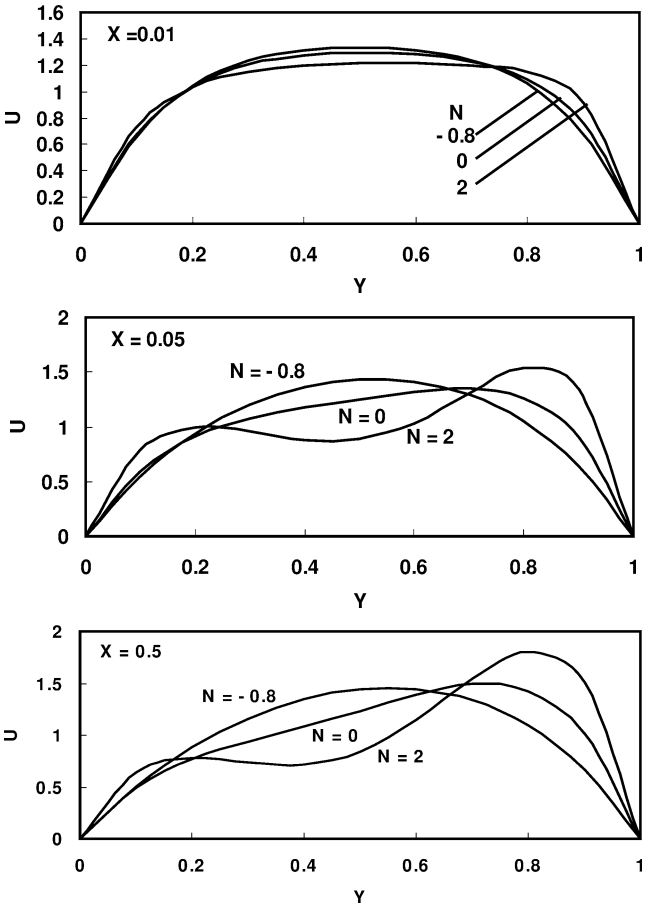

Fig. 2. Effect of N on the velocity profiles. ($Pr = Sc = 0.7, Gr/Re = 300,\ r_h = r_m = 0.5$).

4.1. Velocity profile

The effects of the buoyancy ratio N on the velocity profiles at different locations are shown in Fig. 2. For pure convection in the channel, the buoyancy forces disappear and the velocity profile takes a parabolic shape with a maximum velocity point is in the middle of the channel. When $N = 0$ the buoyancy force is due to the thermal diffusion only which causes an increase in the velocity near the hot plate. So, the maximum velocity point moves towards the hot plate. Positive N causes additional increase in the velocity near the hot plate and hence a decrease in the velocity near the cool plate will be attained. The maximum velocity point moves towards the hot plate and the velocity profiles become convex. Negative N means that the increase in the velocity near the hot plate, due to the thermal buoyancy force, decreases due to the mass buoyancy force that acts in the opposite direction. So, the distortion of the velocity profile is reduced and the concavity disappears.

4.2. Pressure gradient

Fig. 3 illustrates the variation of the pressure gradient with distance at different values of the buoyancy ratio N.

From the figure, it is evident that the pressure gradient increases with X. Near the entrance, the pressure gradient is negative and as X increases, it becomes positive. Moreover, the pressure gradient increases linearly at large X. Also, the pressure gradient increases with the increase in the buoyancy ratio N. The inflection point of the pressure (i.e., the point at which the pressure gradient becomes zero) occurs at smaller distance X as N increases.

The thermal buoyancy force increases the velocity near the hot plate and as a result the centerline velocity decreases. The pressure gradient becomes zero at about the point where the centerline velocity starts to decrease. Since positive N causes additional increase in the velocity near the hot plate and consequently, more decreasing in the centerline velocity, it is expected that the pressure gradient becomes zero at smaller distance X. Negative N means that the mass buoyancy force opposes the thermal buoyancy force. Therefore, less decreasing in the centerline velocity is attained and the inflection point occurs at larger X.

4.3. Temperature and concentration profiles

The developments of temperature and concentration at different values of the buoyancy ratio are shown in Fig. 4. From the figure it is clear that the temperature and concentration profiles are less sensitive to the buoyancy ratio than the velocity profiles since the buoyancy ratio affects the velocity directly. For the present case, i.e., uniform heat and mass fluxes, the values of the temperature and concentration increase as X increases. This is due to the addition of constant and continued heat and mass fluxes at the plate. Moreover, temperature and concentration on the hot plate are slightly higher than those on the cool plate because $r_h = r_m = 0.5$ (< 1). Also, positive N decreases, slightly, the temperature and concentration on the hot plate because of the increasing in the velocity near this plate. Conversely, negative N increases, slightly, the temperature and concentration on the hot plate because of the decreasing in the velocity near this plate.

4.4. Heat and mass transfer

The effect of the buoyancy ratio on the local Nusselt number (Sherwood number) on the hot plate is shown in Fig. 5. The figure reveals that the Nusselt number increases when the mass buoyancy force acts in the same direction as the thermal buoyancy force (i.e., $N > 0$). Negative N decreases the velocity near the hot plate and hence Nu_1 becomes less. At large X, these effects diminish.

Fig. 6 illustrates the effect of the thermal buoyancy force on the local Nusselt number Nu_1 (Sh_1). As shown from the figure, the Nusselt number increases as Gr/Re increase. This

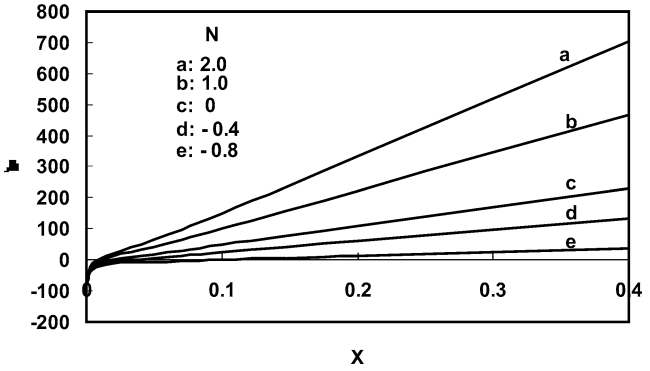

Fig. 3. Effect of N on the pressure gradient. ($Pr = Sc = 0.7, Gr/Re = 300,\ r_h = r_m = 0.5$).

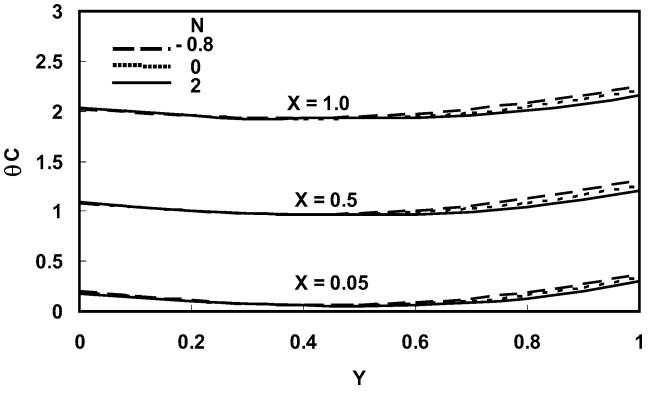

Fig. 4. Developments of temperature and concentration profiles. ($Pr = Sc = 0.7,\ Gr/Re = 300,\ r_h = r_m = 0.5$).

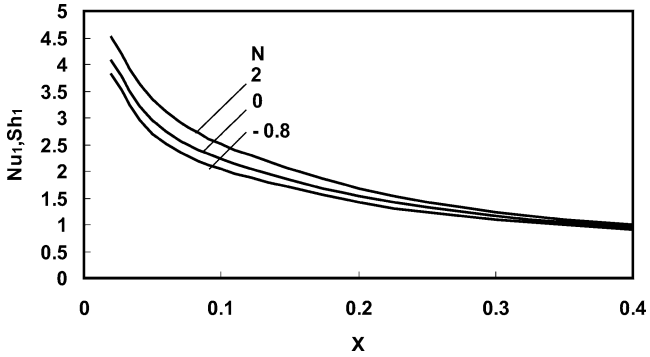

Fig. 5. Effect of N on Nu_1 (Sh_1). ($Pr = Sc = 0.7, Gr/Re = 300,\ r_h = r_m = 0.5$).

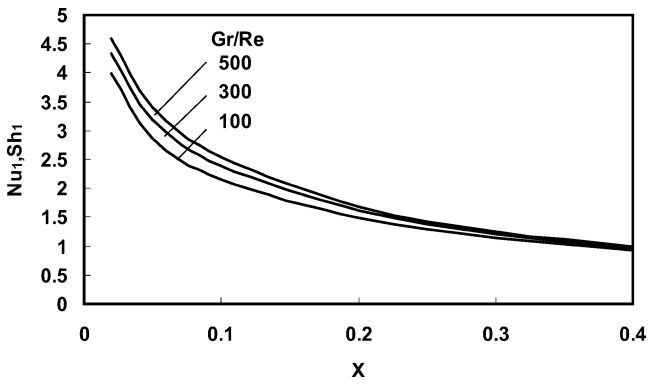

Fig. 6. Effect of Gr/Re on Nu_1 (Sh_1). ($Pr = Sc = 0.7, r_h = r_m = 0.5,\ N = 1$).

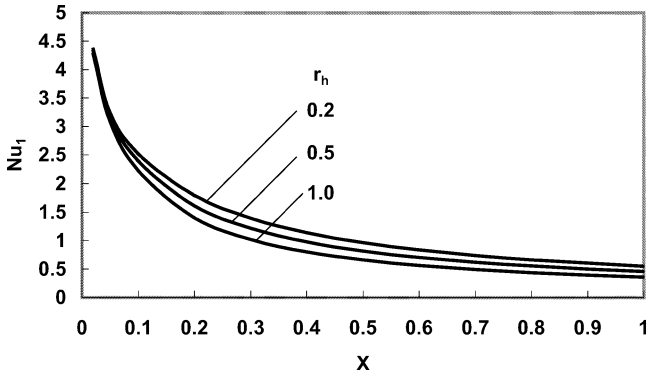

Fig. 7. Effect of r_h on Nu_1. ($Pr = Sc = 0.7$, $Gr/Re = 300$, $r_m = 0.5$, $N = 1$.)

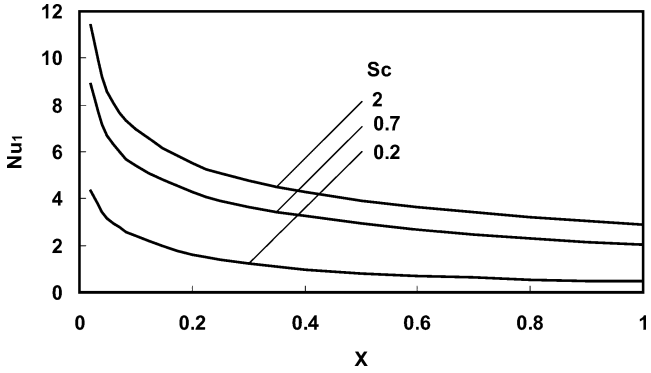

Fig. 8. Effect of Sc on Nu_1. ($Pr = 0.7$, $Gr/Re = 300$, $r_h = r_m = 0.5$, $N = 1$.)

is due to the increase in the velocity near the hot plate as a result of the increasing of the thermal buoyancy force. At large X, this effect diminishes.

The effect of the heat flux ratio r_h on the local Nusselt number Nu_1 is shown in Fig. 7. From the figure it is clear that the Nusselt number for the case of symmetric heating ($r_h = 1$) is smaller than that for the case of asymmetric heating ($r_h < 1$). Asymmetric heating decreases the temperature near the hot plate. Consequently, the Nusselt number increases on the hot plate. This effect is insignificant near the inlet. The effect of r_m on the local Sherwood number Sh_1 is similar to the effect of r_h on the local Nusselt number Nu_1.

The effect of Schmidt number on the local Sherwood number Sh_1 is shown in Fig. 8. It is clearly seen that a larger Sc results in a larger Sh_1. This is due to that as Sc becomes larger, the concentration boundary layer thickness becomes thinner relative to the flow boundary layer thickness. So, the rate of mass transfer increases. Consequently, the Sherwood number increases.

5. Conclusion

The development of laminar convection between two vertical parallel plates with thermal and mass buoyancy forces has been investigated numerically. The plates have different uniform heat and mass fluxes. A parametric study has been carried out to evaluate the influence of the various parameters on heat and mass transfer between the plates. It can be concluded that:

(1) The temperature and concentration profiles are less sensitive to the buoyancy ratio N than the velocity profiles. For positive N, the velocity profiles are highly distorted by the mass buoyancy force.
(2) The pressure gradient increases with distance within the channel. At large X, this increasing is linear. The pressure gradient is also increases with the increase in the buoyancy ratio.
(3) Positive N increases the Nusselt number and Sherwood number while negative N decreases them. Increasing of the thermal buoyancy force increases both of them.
(4) Decreasing of the heat flux ratio and the mass flux ratio increases the Nusselt number and Sherwood number.
(5) Large Sc increases the rate of mass transfer between the plates.

References

[1] R. Bodoia, J.F. Osterle, The development of free convection between heated vertical plates, ASME J. Heat Transfer 84 (1962) 40–44.
[2] W. Aung, L.S. Fletcher, V. Sernas, Developing laminar free convection between vertical flat plates with asymmetric heating, Internat. J. Heat Mass Transfer 15 (1972) 2293–2308.
[3] O. Miyatake, T. Fujii, Natural convection heat transfer between vertical parallel plates at unequal uniform temperatures, Heat Transfer Japan. Res. 2 (1973) 79–88.
[4] O. Miyatake, T. Fujii, Natural convection heat transfer between vertical parallel plates with unequal heat fluxes, Heat Transfer Japan. Res. 3 (1974) 29–33.
[5] H. Akbari, T.R. Borgers, Free convective laminar flow within the Trombe wall channel, Solar Energy 22 (1979) 165–174.
[6] W. Aung, G. Worku, Developing flow and flow reversal in a vertical channel with asymmetric wall temperatures, ASME J. Heat Transfer 108 (1986) 299–304.
[7] S. Habchi, S. Acharya, Laminar mixed convection in a symmetrically or asymmetrically heated vertical channel, Numer. Heat Transfer 9 (1986) 605–618.
[8] D.B. Ingham, D.J. Keen, P.J. Heggs, Flow in vertical channels with asymmetric wall temperatures and including situations where reverse flows occur, ASME J. Heat Transfer 110 (1988) 910–917.
[9] E. Darie, S. Kimura, A. Okajima, Natural convection heat transfer in an asymmetrically heated vertical channel controlled by through flows, JSME Ser. B 41 (1998) 227–232.
[10] L.N. Tao, On combined free and forced convection in channels, ASME J. Heat Transfer 82 (1960) 233–238.
[11] W. Aung, Fully developed laminar free convection between vertical plates heated asymmetrically, Internat. J. Heat Mass Transfer 15 (1972) 1577–1580.
[12] W. Aung, G. Worku, Theory of fully developed, combined convection including flow reversal, ASME J. Heat Transfer 108 (1986) 485–488.
[13] C.H. Cheng, H.S. Kou, W.H. Huang, Flow reversal and heat transfer of fully developed mixed convection in vertical channels, J. Thermophys. Heat Transfer 4 (1990) 375–383.
[14] T.T. Hamadah, R.A. Wirtz, Analysis of laminar fully developed mixed convection in a vertical channel with opposing buoyancy, ASME J. Heat Transfer 113 (1991) 507–510.

[15] R.A. Wirtz, R.J. Stutzman, Experiments on free convection between vertical plates with symmetric heating, ASME J. Heat Transfer 104 (1982) 501–507.
[16] E.M. Sparrow, G.M. Chrysler, L.F. Azevedo, Observed flow reversals and measured-predicted Nusselt numbers for natural convection in a one-sided heated vertical channel, ASME J. Heat Transfer 106 (1984) 325–332.
[17] D.J. Nelson, B.D. Wood, Combined heat and mass transfer natural convection between vertical parallel plates, Internat. J. Heat Mass Transfer 32 (1989) 1779–1787.
[18] D.J. Nelson, B.D. Wood, Combined heat and mass transfer natural convection between vertical parallel plates with uniform flux boundary conditions, Heat Transfer 4 (1986) 1587–1592.
[19] D.J. Nelson, B.D. Wood, Fully developed combined heat and mass transfer natural convection between vertical parallel plates with asymmetric boundary conditions, Internat. J. Heat Mass Transfer 32 (1989) 1789–1792.
[20] T.S. Lee, P.G. Parikh, A. Acrivos, D. Bershader, Natural convection in a vertical channel with opposing buoyancy forces, Internat. J. Heat Mass Transfer 25 (1982) 499–511.
[21] W.M. Yan, T.F. Lin, C.J. Chang, Combined heat and mass transfer in natural convection vertical parallel plates, Warme-und Stoffubertragung 23 (1988) 69–76.
[22] G. Desrayaud, G. Lauriat, Heat and mass transfer analogy for condensation of humid air in vertical channel, Heat Mass Transfer 37 (2001) 67–76.
[23] W.M. Yan, T.F. Lin, Combined heat and mass transferin natural convection between vertical parallel plates with film evaporation, Internat. J. Heat Mass Transfer 33 (1990) 529–541.
[24] W.M. Yan, Effects of film evaporation on laminar mixed convection heat and mass transfer in a vertical channel, Internat. J. Heat Mass Transfer 35 (1992) 3419–3429.
[25] A.A. Cherif, A. Daif, Etude numerique du transfert de chaleur et de masse entre deux plaques planes verticals en presence d'un film de liquide binaire ruisselant sur l'une des plaques chauffee, Internat. J. Heat Mass Transfer 42 (1999) 2399–2418.
[26] K.T. Lee, Natural convection heat and mass transfer in partially heated vertical parallel plates, Internat. J. Heat Mass Transfer 42 (1999) 4417–4425.
[27] M.M. Salah El-Din, Fully developed forced convection in a vertical channel with combined buoyancy forces, Internat. Comm. Heat Mass Transfer 19 (1992) 239–248.
[28] W.M. Yan, Transport phenomena of developing laminar mixed convection heat and mass transfer in inclined rectangular ducts, Internat. J. Heat Mass Transfer 38 (1995) 2905–2914.